Energy spectrum and size quantization in partially ordered semiconductor alloys

M. E. Raikh and E. V. Tsiper*
Department of Physics, University of Utah, Salt Lake City, Utah 84112
(Received 3 June 1993; revised manuscript received 23 August 1993)

We present the analytical theory for the conduction-band spectrum in partially ordered semiconductor alloys. It is assumed that the ordering causes the coupling of the electronic states of Γ minimum with the states of the closest-in-energy L minimum only. We analyze the reduction of the band gap, change of the effective mass, nonparabolicity, and anisotropy of the electronic spectrum, caused by ordering. Using the spectrum obtained we study the size quantization in an ordered domain sandwiched between two disordered regions. We also calculate the electronic spectrum in the region of interpenetration of two variants of ordering along the $[\bar{1}11]$ and $[1\bar{1}1]$ directions. The localization of an electron in such a region is studied.

I. INTRODUCTION

Spontaneous long-range ordering in mixed semiconductor alloys has recently become the object of intensive study. In the ordered phase of a compound $A_xB_{1-x}C$ the cation sublattice represents a system of alternating planes predominantly occupied by type A and type B atoms. The same also applies to the alloys with anion substitution.

The observation of ordering has been reported for nearly all III-V ternary [$In_xGa_{1-x}As$,[1–4] $Ga_xAs_{1-x}P$,[4–8] and $In_xAs_{1-x}Sb$ (Refs. 4 and 9], $In_xAs_{1-x}P$,[4,10] $Ga_xAl_{1-x}As$,[11,12] $In_xAl_{1-x}As$,[4,13] $Ga_xP_{1-x}Sb$,[4,14] $In_xP_{1-x}Sb$,[4,14] $Ga_xAs_{1-x}Sb$,[4,15] and quaternary [$In_xAl_{1-x}Ga_yP_{1-y}$ (Refs. 4 and 16) and $In_xGa_{1-x}As_yP_{1-y}$ (Refs. 2, 3, and 8)] alloys. Most of the works, however, investigate the ordering in $In_xGa_{1-x}P$ with $x \approx 0.5$.[4,17–25]

The experimental studies of ordered materials are being conducted in the following directions: (i) The investigation of atomic structure of ordered alloys by transmission electron microscopy (TEM) and x-ray analysis, (ii) the optical study of electronic properties, and (iii) the use of ordered materials for device design. The TEM experiments indicate that the ordering of CuPt type occurs in two variants: with the axis along the $[\bar{1}11]$ and $[1\bar{1}1]$ directions.[3,7–10] Moreover, these two variants may coexist within one sample. Structural studies also show that the ordered regions form a domain-like structure within a disordered matrix.[3–8,17]

Photoluminescence studies indicate that the ordering leads to a splitting of the valence band which, in turn, manifests itself in the polarization of emitted light.[26–29] However, the major effect is a considerable ordering-induced reduction of the band gap, revealed both in luminescence[28–33] and electroreflectance[34–36] experiments.

To our knowledge the first device applications of ordered materials were reported in Refs. 37 and 38. Lee, Horng, and Haung[37] made use of the fact that the degree of ordering and hence the width of the band gap are functions of the growth temperature. By changing the temperature during the growing process they created a potential well in the form of the ordered layer sandwiched between disordered ones. This potential well worked as a visible light-emitting diode. Also, the fabrication of a semiconductor laser with ordered $In_xGa_{1-x}P$ active region was reported in Ref. 38.

The formation of ordering was studied theoretically in a number of papers.[39–48] Zunger and co-workers[39–45] have performed the detailed investigation of the thermodynamic stability of ordered alloys. They have predicted a few ordering configurations to be more stable than the random distribution.[39,40] The same authors have also studied the role of the surface for the formation of ordering in the growing process.[41–43]

The band-gap reduction due to ordering was reproduced in numerical calculations.[48–53] The qualitative reason for gap lowering is believed to be as follows. Ordering couples electronic states in the center and at the boundary of the Brillouin zone. In particular, in the case of CuPt ordering the Γ and L points are coupled. Such a coupling causes the repulsion of Γ and L minima in $\mathbf{k}$ space.[48–50] As a result the bottom of the conduction band moves down. Ordered $In_xGa_{1-x}P$ is known to exhibit strong band-gap reduction as compared to other III-V solid solutions. This property should be attributed to the anomalously small energy distance between Γ and L conduction-band minima ($\approx$ 100 meV) in the disordered phase of this material.

Previous calculations of electronic structure were focused on the band edge positions in the ordered phase.[48–51] The consequences of ordering for the electronic spectrum were not studied. In the present paper we develop the elementary theory of the conduction-band spectrum, based on the idea of band repulsion. Our theory predicts strong nonparabolicity of the conduction band, a perceptible increase in the electron effective mass, and the appearance of its anisotropy caused by the anisotropy of the L valley. Ordering enters in the theory through only one parameter—the strength of Γ-L coupling, which can be found from the experimental value of band-gap reduction. We express all characteristics of the electronic spectrum using this parameter and the band

structure of the random alloy.

Unfortunately, the conventional way to study the electronic spectrum using magneto-optics and cyclotron resonance is strongly impeded in $In_xGa_{1-x}P$ ordered alloys having low mobility and a relatively large band gap. For this reason we apply our results to the problem of size quantization in a quantum well caused by ordering. Since the energy-level positions obtained are quite different from those for a conventional quantum well, the experimental study of size quantization can be the direct test for the applicability of our theory. Note, however, that the ordering-induced potential wells studied up to now[37] were too wide for size quantization to be relevant.

Another question we address in the present paper is the effect of interpenetration of two variants of ordering on the electronic spectrum. The TEM data do not allow one to judge the presence of the regions in which two variants overlap in the samples studied. From the point of view of the atomic configuration such an overlap is not forbidden. We show it with a concrete example of the distribution of atoms over the lattice sites. We also show that the interpenetration of two variants of ordering results in an additional reduction of the band gap as compared to a single variant. Therefore, the region of overlapping represents a quantum well. We study the size quantization in such a well as a function of its thickness and the degree of ordering.

The paper is organized as follows. In Sec. II the dispersion relation for the conduction band in the ordered material is derived. In Sec. III we calculate the positions of the energy levels in one-dimensional quantum well constituted by an ordered domain, sandwiched between two disordered regions. In Sec. IV we study the size quantization in the region of overlapping of two variants of ordering. Section V concludes the paper.

II. CONDUCTION-BAND SPECTRUM OF PARTIALLY ORDERED ALLOY

Consider, for example, an alloy with cation substitution $A_xB_{1-x}C$. The conventional approach to the calculation of the band structure is the so-called "virtual-crystal approximation." In the frame of this approach the true potential of the cation sublattice

$$\Phi_0(\mathbf{r}) = \sum_i c_i \mathcal{V}_A(\mathbf{r}-\mathbf{r}_i) + (1-c_i)\mathcal{V}_B(\mathbf{r}-\mathbf{r}_i) \qquad (1)$$

is replaced by the periodic potential

$$\overline{\Phi_0(\mathbf{r})} = \sum_i x\mathcal{V}_A(\mathbf{r}-\mathbf{r}_i) + (1-x)\mathcal{V}_B(\mathbf{r}-\mathbf{r}_i), \qquad (2)$$

$\mathcal{V}_A$ and $\mathcal{V}_B$ being the potentials of atoms A and B, respectively. In Eq. (1) the coefficients c_i take the values of unity or zero depending on which atom A or B occupies the site i. In Eq. (2) these coefficients are replaced by their average value $\overline{c_i} = x$. Such a replacement implies the equivalency of the all cation-lattice sites.

In the case of ordering the cation sublattice is divided into two sub-sublattices rich with type A and type B atoms, respectively, while all sites within each sub-sublattice can be still treated as equivalent. Then the potential of cation sublattice should be written as

$$\Phi(\mathbf{r}) = \sum_i c_i \mathcal{V}_A(\mathbf{r}-\mathbf{r}_i) + (1-c_i)\mathcal{V}_B(\mathbf{r}-\mathbf{r}_i) + \sum_j d_j \mathcal{V}_A(\mathbf{r}-\mathbf{r}_j) + (1-d_j)\mathcal{V}_B(\mathbf{r}-\mathbf{r}_j), \qquad (3)$$

where the summation is performed over sites i of the first and sites j of the second sub-sublattices. Ordering means that $\overline{c_i} \neq \overline{d_j}$.

The average composition x is related to $\overline{c_i}$ and $\overline{d_j}$ as

$$x = \frac{\overline{c_i} + \overline{d_j}}{2}. \qquad (4)$$

We define the ordering parameter ν as

$$\nu = \frac{|\overline{c_i} - \overline{d_j}|}{2x}, \qquad (5)$$

so that ν is zero for the disordered phase while $\nu = 1$ corresponds to the strongest possible ordering at a given composition x.

After averaging of (3) we get the following form for the virtual-crystal potential in the presence of ordering:

$$\overline{\Phi(\mathbf{r})} = \sum_i [x(1+\nu)]\mathcal{V}_A(\mathbf{r}-\mathbf{r}_i) + [1-x(1+\nu)]\mathcal{V}_B(\mathbf{r}-\mathbf{r}_i) + \sum_j [x(1-\nu)]\mathcal{V}_A(\mathbf{r}-\mathbf{r}_j) + [1-x(1-\nu)]\mathcal{V}_B(\mathbf{r}-\mathbf{r}_i)\ . \qquad (6)$$

The symmetry of this potential corresponds to the doubling of the period in the direction of ordering. The perturbation $\overline{\delta\Phi(\mathbf{r})} = \overline{\Phi(\mathbf{r})} - \Phi_0(\mathbf{r})$ caused by ordering takes the form

$$\overline{\delta\Phi(\mathbf{r})} = \nu x \left[\sum_i \mathcal{V}(\mathbf{r}-\mathbf{r}_i) - \sum_j \mathcal{V}(\mathbf{r}-\mathbf{r}_j) \right], \qquad (7)$$

where $\mathcal{V}(\mathbf{r}) = \mathcal{V}_A(\mathbf{r}) - \mathcal{V}_B(\mathbf{r})$ is the difference between the A and B atomic potentials.

Let a be the period of the unperturbed potential (1) in the direction of ordering. We also introduce the wave vector $\boldsymbol{\sigma}$ directed along the axis of ordering with the length $|\boldsymbol{\sigma}| = \pi/a$. Then the potential (7) can be presented in the form

$$\overline{\delta\Phi(\mathbf{r})} = \nu x e^{i\boldsymbol{\sigma}\cdot\mathbf{r}} P(\mathbf{r})\ , \qquad (8)$$

where

$$P(\mathbf{r}) = \sum_i e^{-i\boldsymbol{\sigma}\cdot(\mathbf{r}-\mathbf{r}_i)} \mathcal{V}(\mathbf{r}-\mathbf{r}_i) \qquad (9)$$

is the periodic function with the periodicity of the unperturbed lattice. Summation in (9) is performed over all sites of the cation sublattice.

For concreteness we will consider the ordering of CuPt type. In this case the potential $\delta\Phi$ couples electronic states of the Γ minimum with electronic states of, generally speaking, all energy minima at the L point of the Brillouin zone.

The main assumption we will adopt is that the coupling occurs mainly with the L minimum closest in energy to the Γ point. This implies that the energy distance W (see Fig. 1) is much smaller than the energy distance to the next L minimum. This assumption is justified for most wide-gap III-V compounds. For example, in the case of $In_{1-x}Ga_xP$ with $x \approx 0.5$ according to the band-structure data[54] we have $W = 120$ meV while the distance to the next L minimum exceeds 3 eV. This allows a search for the wave function in the conduction band of the ordered phase in the form

$$\Psi_{\mathbf{k}}(\mathbf{r}) = e^{i\mathbf{k}\cdot\mathbf{r}}\left[u_{\Gamma\mathbf{k}}(\mathbf{r}) + \lambda_{\mathbf{k}} e^{-i\boldsymbol{\sigma}\cdot\mathbf{r}} u_{L\mathbf{k}-\boldsymbol{\sigma}}(\mathbf{r})\right]. \tag{10}$$

Here $u_{\Gamma\mathbf{k}}$ and $u_{L\mathbf{k}}$ are the Bloch amplitudes of the Γ and L minima, respectively; $\lambda_{\mathbf{k}}$ is the coupling coefficient. The combination in the square brackets represents the corresponding Bloch amplitude for the ordered phase.

The energy spectrum $E_{\mathbf{k}}$ should be found from the solution of the Schrödinger equation

$$\left[\frac{\hat{\mathbf{p}}^2}{2m_0} + \overline{\Phi_0(\mathbf{r})} + \overline{\delta\Phi(\mathbf{r})}\right]\Psi_{\mathbf{k}} = E_{\mathbf{k}}\Psi_{\mathbf{k}}, \tag{11}$$

where $\hat{\mathbf{p}}$ is the momentum operator and m_0 is the free electron mass. Substituting (10) into (11), multiplying alternately by $u^*_{\Gamma\mathbf{k}}$ and $u^*_{L\mathbf{k}-\boldsymbol{\sigma}}$, and integrating over the volume we obtain the following system:

$$[\varepsilon_\Gamma(\mathbf{k}) - E(\mathbf{k})] + \lambda_{\mathbf{k}} V = 0, \tag{12a}$$

$$\lambda_{\mathbf{k}}[\varepsilon_L(\mathbf{k}) - E(\mathbf{k})] + V^* = 0, \tag{12b}$$

where the functions $\varepsilon_\Gamma(\mathbf{k})$ and $\varepsilon_L(\mathbf{k})$ are defined as

$$\varepsilon_\Gamma(\mathbf{k}) = \frac{\hbar^2\mathbf{k}^2}{2m_\Gamma}, \quad \varepsilon_L(\mathbf{k}) = W + \frac{\hbar^2 k_\parallel^2}{2m_{L\parallel}} + \frac{\hbar^2 k_\perp^2}{2m_{L\perp}}, \tag{13}$$

$\varepsilon_\Gamma(\mathbf{k})$ being the energy spectrum of Γ minimum with the effective mass m_Γ; $k_\parallel$ and $k_\perp$ are the components of the vector $\mathbf{k}$ parallel and perpendicular to the direction of ordering; $m_{L\parallel}$ and $m_{L\perp}$ are, respectively, the longitudinal and transverse effective masses in the L minimum. Note that the energy spectrum of L minimum is given by $\varepsilon_L(\mathbf{k} - \boldsymbol{\sigma})$. The coupling parameter V is defined as

$$V = \nu x \int d\mathbf{r}\, u^*_{\Gamma\mathbf{k}} P(\mathbf{r}) u_{L\mathbf{k}-\boldsymbol{\sigma}}. \tag{14}$$

The energy spectrum obtained from (12) has the form

$$E_\pm(\mathbf{k}) = \frac{\varepsilon_\Gamma(\mathbf{k}) + \varepsilon_L(\mathbf{k})}{2} \pm \sqrt{\left(\frac{\varepsilon_\Gamma(\mathbf{k}) - \varepsilon_L(\mathbf{k})}{2}\right)^2 + V^2}. \tag{15}$$

Here and in what follows, for simplicity of notation, we denote by V the absolute value of the matrix element (14).

This formula describes two branches of the conduction-band spectrum shown schematically in Fig. 1. At $\mathbf{k} = 0$ it gives the value of ordering-induced band-gap reduction

$$\delta E = \sqrt{\left(\frac{W}{2}\right)^2 + V^2} - \frac{W}{2}. \tag{16}$$

The main consequence of Eq. (14) is the significant change in the electron effective mass due to ordering. Another consequence is the anisotropy of the conduction band originating from the anisotropy of $\varepsilon_L(\mathbf{k})$. Expanding (15) at small $\mathbf{k}$ we obtain for the longitudinal and transverse effective masses of the lower branch E_-

$$\frac{1}{m^-_{\parallel,\perp}} = \frac{1}{2m_\Gamma}\left[1 + \frac{W}{\sqrt{W^2 + 4V^2}}\right] + \frac{1}{2m_{L\parallel,\perp}}\left[1 - \frac{W}{\sqrt{W^2 + 4V^2}}\right]. \tag{17}$$

The analogous expression for the upper branch E_+ reads

$$\frac{1}{m^+_{\parallel,\perp}} = \frac{1}{2m_\Gamma}\left[1 - \frac{W}{\sqrt{W^2 + 4V^2}}\right] + \frac{1}{2m_{L\parallel,\perp}}\left[1 + \frac{W}{\sqrt{W^2 + 4V^2}}\right]. \tag{18}$$

The ratio $m_\parallel/m_\perp$ for both branches can be written as

$$\frac{m^\pm_\parallel}{m^\pm_\perp} = \left(\frac{m_{L\parallel}}{m_{L\perp}}\right)\frac{m_\Gamma + m_{L\perp}\left[\sqrt{\left(\frac{W}{2V}\right)^2 + 1} \mp \frac{W}{2V}\right]^2}{m_\Gamma + m_{L\parallel}\left[\sqrt{\left(\frac{W}{2V}\right)^2 + 1} \mp \frac{W}{2V}\right]^2}. \tag{19}$$

In the limit $m_L \gg m_\Gamma$ the electronic spectrum (15) reduces to

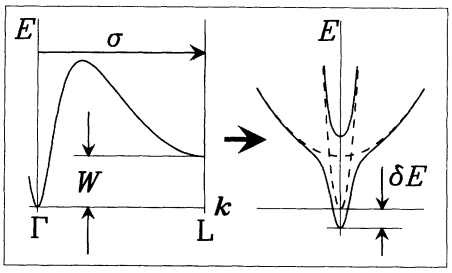

FIG. 1. Schematic illustration of the Γ-L splitting caused by ordering. Left, energy spectrum of the conduction band without ordering; right, same spectrum in the presence of ordering.

$$E_-(k) = \frac{1}{2}\left\{ W + \frac{\hbar^2 k^2}{2m_\Gamma} - \sqrt{\left(W - \frac{\hbar^2 k^2}{2m_\Gamma}\right)^2 + 4V^2} \right\} \tag{20}$$

and does not contain the effective mass of the L minimum, which is not known exactly. In the same limit Eqs. (17) and (18) can be simplified to

$$m^{\pm} = 2m_\Gamma \sqrt{\left(\frac{W}{2V}\right)^2 + 1}\left[\sqrt{\left(\frac{W}{2V}\right)^2 + 1} \pm \frac{W}{2V}\right]. \tag{21}$$

We see that in this case the masses in both branches are isotropic and independent of m_L. The maximal value of the effective mass for the lower branch is achieved for $V \gg W$ and is equal to $2m_\Gamma$.

Let us perform the numerical estimates. As mentioned above for $In_{1-x}Ga_xP$ with $x = 0.5$ the energy distance $W \approx 120$ meV. The maximal reported value of δE in this compound is 140 meV.[21] With these values we obtain from Eq. (16) $V \approx 190$ meV. Estimating the effective mass $m_{L\|}$ from the dispersion curves[54] as $m_{L\|} = 20m_\Gamma$ we obtain from (16) $m_\|^- \approx 1.5m_\Gamma$. Such a change should manifest itself in the magneto-optics experiments as well as in the change of binding energy of shallow impurities.

To estimate the anisotropy (19) of the effective mass one needs to know the anisotropy of the L valley. We could not find these data in literature. Taking, for example, $m_{L\|}/m_{L\perp} = 5$, we obtain $(m_\|^- - m_\perp^-)/m_\Gamma \approx 0.14$. Though the anisotropy is small, it could be easily observed in the cyclotron resonance experiment. However, as mentioned in the Introduction, such an experiment is difficult to perform in the wide-gap compounds.

The electronic spectrum $E_-(\mathbf{k})$ is strongly nonparabolic. The expansion of (20) at small k gives

$$E_-(k) = -\delta E + \frac{\hbar^2 k^2}{2m_-}\left(1 - \frac{k^2}{k_0^2}\right), \tag{22}$$

where

$$k_0^2 = \frac{4m_- V}{\hbar^2}\sqrt{\left(\frac{W}{2V}\right)^2 + 1}\left[\frac{W}{2V} + \sqrt{\left(\frac{W}{2V}\right)^2 + 1}\right]^2. \tag{23}$$

We see that nonparabolicity becomes important starting from $k \sim k_0$, which is much smaller than $\sqrt{m_\Gamma E_g}$—the characteristic value in the absence of ordering, E_g being the energy gap.

In Fig. 2(a) we show the calculated dependences $E_\pm(k)$ for different ratios m_L/m_Γ. It is seen that the spectrum (23) is a good approximation already for $m_L \sim 10m_\Gamma$. For the upper branch the spectrum does not change with m_L already for $m_L > 3m_\Gamma$. Figure 2(b) shows the evolution of the energy spectrum with increasing ordering parameter. We see that in the vicinity of $\mathbf{k} = 0$ the upper and lower branches are almost parallel to each other for large ordering parameter. It means that if the absorption of light between these two branches is studied the absorption spectrum will represent a very narrow peak.

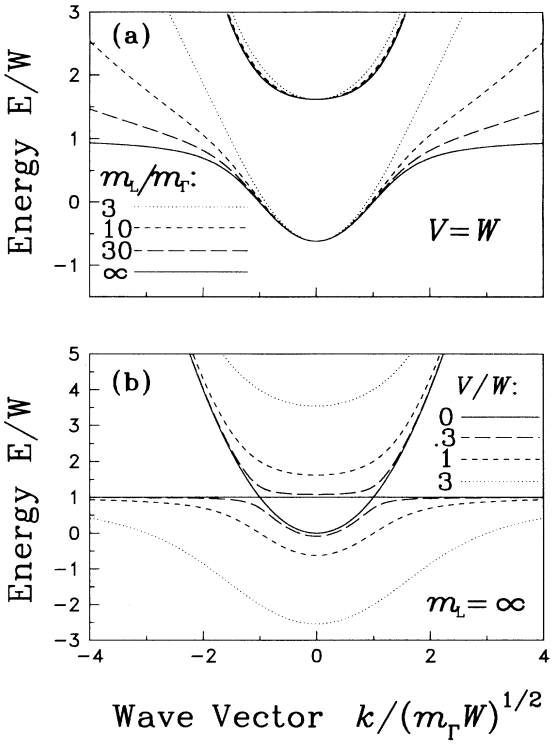

FIG. 2. Energy spectrum of the conduction band of ordered alloy as defined by Eq. (15) for (a) $V = W$ and different ratios of the effective masses in L and Γ minima and (b) in the limit $m_L \to \infty$ for different degrees of ordering.

In conclusion of the section let us discuss the validity of the approach employed. Although we derive the form of the ordering-induced perturbation (8) using the virtual-crystal approximation, in fact formula (8) is general if we understand by $P(\mathbf{r})$ some periodic function with the periodicity of the unperturbed lattice. Since this function appears only in the expression (14) for the parameter V, which is supposed to be determined from the experimental data, the dispersion relation (15) [as well as (20)] for the electronic spectrum in the ordered phase is also general. Correspondingly, the consequences we draw from these equations (nonparabolicity, anisotropy, and the change in the electron effective mass) are not specific for the virtual-crystal approximation.

There is another point worth discussion. Namely replacing an alloy by the equivalent crystal one neglects the effects caused by compositional fluctuations. These effects are the smearing of the band edge, resulting from the alloy scattering, and the fluctuation-induced shift of the band edge. Both effects are discussed in the review in Ref. 55.

For an alloy with composition x the smearing is small and proportional to $x^2(1-x)^2$ while the shift, being larger than the smearing, is proportional to $x(1-x)$ (see, e.g., Ref. 55). This shift provides a contribution to the bowing parameter. To our knowledge, the role of this contribution in the experimental values of the bowing parameter is not well established by now. In other words,

it is not known whether the compositional dependence of the equivalent periodic crystal already gives the major contribution to the bowing or it comes mainly from the fluctuation-induced shift. Indeed, the ordering suppresses the statistical fluctuations and thus diminishes the contribution of the disorder to the shift of the band edge.

Actually we can relate the shifts in the disordered and in the ordered phases to each other. Let us denote with $x(1-x)\Delta$ the shift in the disordered alloy with composition x. Assuming the random distribution of the atoms in the planes, perpendicular to the ordering axis, it can be shown that the corresponding shift in the ordered phase is equal to $x[1-x(1+\nu^2)]\Delta$, ν being the ordering parameter (5). In particular, for $x=0.5$ and $\nu=1$ we have a superlattice without any disorder, so that the shift is zero. We also see that the relative decrease of the shift, caused by ordering, is $x\nu^2/(1-x)$. This means that, strictly speaking, the band-edge position in Eq. (13) is measured from the energy $x^2\nu^2\Delta$ above the actual value in the disordered phase. However, such a shift does not affect the shape of the electronic spectrum, shown in Figs. 1 and 2.

III. SIZE QUANTIZATION IN AN ORDERED DOMAIN

In this section we calculate the positions of size quantization levels in a plane ordered domain sandwiched between two disordered regions. The band diagram of the structure we study is shown schematically in Fig 3. It is easy to see that when the band-gap reduction δE is much smaller than the Γ-L energy distance W, i.e., in the case of weak ordering, the problem just reduces to the usual size quantization in a potential well of width d and depth δE.

If, however, the ordering is not small, so that $\delta E \sim W$, both branches participate in the formation of the size quantization wave functions inside the well. Correspondingly, the wave functions outside the well ($|x| > d/2$) should be chosen as a combination of the Bloch functions of Γ and L minima multiplied by envelope functions decaying with $|x|$. The problem is therefore to match the inner and outer envelope functions together with their derivatives at the boundaries $x = \pm d/2$.

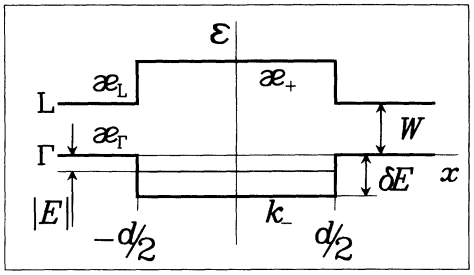

FIG. 3. Schematic band profile in the quantum well formed by ordered domain sandwiched between disordered regions. The position E of the size quantization level is measured from the bottom of the Γ minimum in the disordered material.

It is obvious that the wave functions of the all size quantization levels are either even or odd. For even size quantization levels the wave function outside the well $|x| > d/2$ has the form

$$\Psi(\mathbf{r}) = D_\Gamma e^{-æ_\Gamma|x|}u_\Gamma(\mathbf{r}) + D_L e^{-æ_L|x|}e^{i\sigma\cdot\mathbf{r}}u_L(\mathbf{r}), \quad (24)$$

where the decay constants $æ_\Gamma$ and $æ_L$ are equal to

$$æ_\Gamma = \frac{1}{\hbar}\sqrt{2m_\Gamma|E|}, \quad (25a)$$

$$æ_L = \frac{1}{\hbar}\sqrt{2m_L(W+|E|)}. \quad (25b)$$

For an even level the wave function inside the well has the form

$$\Psi(\mathbf{r}) = C_-\cos(k_-x)[u_\Gamma(\mathbf{r}) + \lambda_{k_-}e^{i\sigma\cdot\mathbf{r}}u_L(\mathbf{r})] + C_+\cos(k_+x)[u_\Gamma(\mathbf{r}) + \lambda_{k_+}e^{i\sigma\cdot\mathbf{r}}u_L(\mathbf{r})], \quad (26)$$

where $k_\pm$ are the solutions of the equations $E_+(k_+) = E$ and $E_-(k_-) = E$ correspondingly. Here E is the sought size quantization energy. The dispersion laws $E_+(k)$ and $E_-(k)$ are defined by Eq. (15). Using the expressions (13) for $\varepsilon_\Gamma(k)$ and $\varepsilon_L(k)$, we obtain

$$k_\pm^2 = -\frac{1}{\hbar^2}\{m_\Gamma|E| + m_L(|E|+W) \pm \sqrt{[m_\Gamma|E| - m_L(|E|+W)]^2 + 4m_\Gamma m_L V^2}\}\,. \quad (27)$$

Here m_L is the effective mass of the L minimum in the x direction. For an odd level one should change the sign of the wave function to the left (or to the right) of the well and replace cos by sin.

The coupling coefficients $\lambda_{k_\pm}$ are to be found substituting $E(k) = E$ into Eq. (12):

$$\lambda_{k_\pm} = \frac{1}{V}\left[E - \frac{\hbar^2k_\pm^2}{2m_\Gamma}\right]. \quad (28)$$

Bound states in the quantum well correspond to the energy E within the interval $-\delta E < E < 0$ (Fig. 3). For such E the value k_-^2 is positive and $k_+^2 = -æ_+^2$ is negative.

Matching the envelope functions and their derivatives at the boundary $x = d/2$ results in the following system for the coefficients C_+, C_-, D_Γ, D_L:

$$C_- \cos\frac{k_- d}{2} + C_+ \cosh\frac{æ_+ d}{2} - D_\Gamma \exp\left(-\frac{æ_\Gamma D}{2}\right) = 0, \tag{29a}$$

$$C_- \lambda_{k_-} \cos\frac{k_- d}{2} + C_+ \lambda_{k_+} \cosh\frac{æ_+ d}{2} - D_L \exp\left(-\frac{æ_L D}{2}\right) = 0, \tag{29b}$$

$$C_- k_- \sin\frac{k_- d}{2} - C_+ æ_+ \sinh\frac{æ_+ d}{2} - D_\Gamma æ_\Gamma \exp\left(-\frac{æ_\Gamma D}{2}\right) = 0, \tag{29c}$$

$$C_- \lambda_{k_-} k_- \sin\frac{k_- d}{2} - C_+ \lambda_{k_+} æ_+ \sinh\frac{æ_+ d}{2} - D_L æ_L \exp\left(-\frac{æ_L D}{2}\right) = 0. \tag{29d}$$

Solving this system we obtain the following equation for energy levels of even states:

$$\lambda_{k_-} \frac{k_- \tan(k_- d/2) - æ_L}{k_- \tan(k_- d/2) - æ_\Gamma} = \lambda_{k_+} \frac{æ_+ \tanh(æ_+ d/2) + æ_L}{æ_+ \tanh(æ_+ d/2) + æ_\Gamma}. \tag{30}$$

The analogous equation for odd states reads

$$\lambda_{k_-} \frac{k_- + æ_L \tan(k_- d/2)}{k_- + æ_\Gamma \tan(k_- d/2)} = \lambda_{k_+} \frac{æ_+ + æ_L \tanh(æ_+ d/2)}{æ_+ + æ_\Gamma \tanh(æ_+ d/2)}. \tag{31}$$

The numerical solutions of Eqs. (30) and (31) for different degrees of ordering V/W and mass ratios m_L/m_Γ are shown in Fig. 4. For comparison we show the positions of energy levels for an electron with mass m_Γ in the regular potential well of the same width d and depth δE.

It is seen that for weak ordering the level positions in the case of ordered domain are close to those for regular well. With increasing of the ordering parameter the levels in the domain are, roughly speaking, two times lower than the levels in the regular well.

We can also see from Fig. 4 that the infinite-m_L limit gives a good approximation beginning from $m_L \simeq 10 m_\Gamma$. In this limit Eqs. (30) and (31) for even and odd states can be simplified to

$$\tan\frac{k_- d}{2} = \frac{æ_\Gamma}{k_-} \tag{32}$$

and

$$\tan\frac{k_- d}{2} = -\frac{k_-}{æ_\Gamma}, \tag{33}$$

respectively, where k_- in the limit $m_L \to \infty$ takes the form

$$k_- = \sqrt{E + \frac{V^2}{W - E}}. \tag{34}$$

In the case of narrow well there is only one shallow level E_1 with $|E_1| \ll \delta E$. In this case Eq. (30) can be solved analytically and yields

$$E_1 = -\frac{m_\Gamma m_L V^4}{4\hbar^4 W} d^4 \left(1 - \frac{2d\sqrt{2m_L W}}{3\hbar}\right). \tag{35}$$

This expression is valid for $d \ll \hbar/\sqrt{2m_L W}$ when the second term in parentheses is much smaller than unity. Note the anomalous behavior of the energy level position

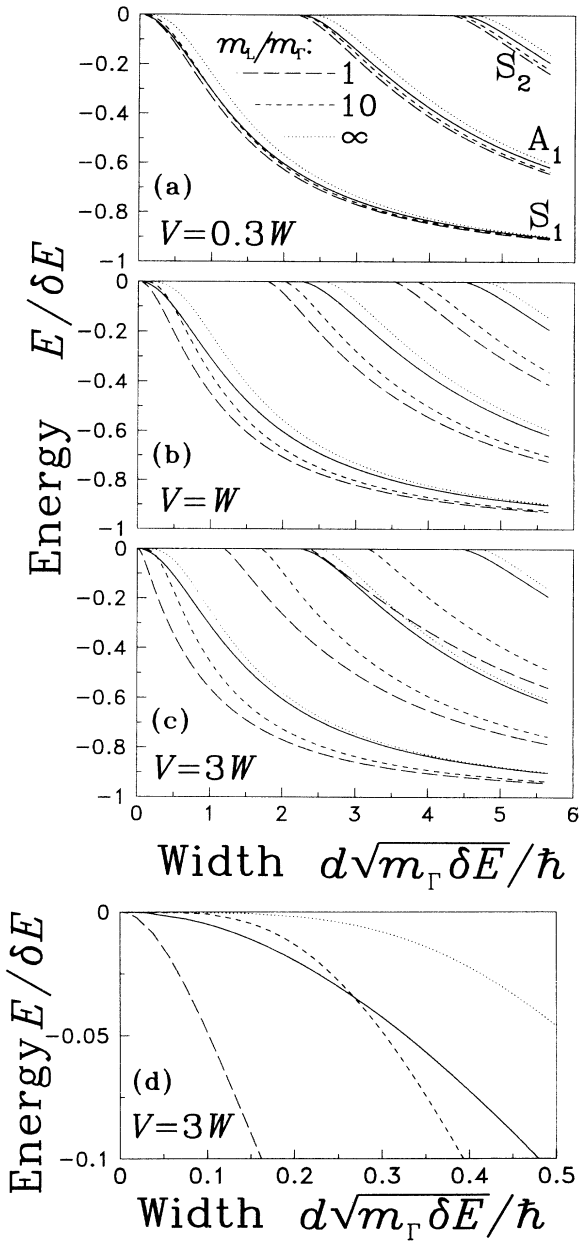

FIG. 4. Energy positions of the first three size quantization levels in the ordered domain, calculated for different mass ratios m_L/m_Γ and degrees of ordering (a) $V = 0.3W$, (b) $V = W$, and (c) $V = 3W$; S and A stand for symmetrical (even) and antisymmetrical (odd) states, respectively. Solid lines show the positions of the energy levels in the regular potential well of the width d and depth δE; (d) the position of the S_1 level, the same as in (c), is shown for the small width of the well.

$|E_1| \propto d^4$. In the case of a regular well one has $|E_1| \propto d^2$. The region of small d, in which the anomalous behavior occurs, is shown in Fig. 4(d).

IV. ENERGY SPECTRUM AND SIZE QUANTIZATION IN THE DOUBLE-ORDERED REGIONS

Consider now a region in which two different variants of ordering coexist. In principle, the formation of such a region can be the result of overlapping of two domains with different variants of ordering. Distribution of atoms in the double-ordered region is illustrated schematically in Fig. 5. Figures 5(a) and 5(b) illustrate single ordering in both variants. The doubled unit cells are shown with dashed lines. The corresponding "chemical formula" for the ordered alloy can be written in the form $(A_{x(1+\nu)}B_{1-x(1+\nu)}C)(A_{x(1-\nu)}B_{1-x(1-\nu)}C)$ instead of ordinary $A_xB_{1-x}C$ for a disordered material. Superposition of Figs. 5(a) and 5(b) results in the double-ordered structure shown in Fig. 5(c). The unit cell of such a structure is doubled twice, so that the chemical formula describing the unit cell reads

$$(A_{x(1+\nu_1+\nu_2)}B_{1-x(1+\nu_1+\nu_2)}C)(A_{x(1+\nu_1-\nu_2)}B_{1-x(1+\nu_1-\nu_2)}C)(A_{x(1-\nu_1+\nu_2)}B_{1-x(1-\nu_1+\nu_2)}C)(A_{x(1-\nu_1-\nu_2)}B_{1-x(1-\nu_1-\nu_2)}C);$$

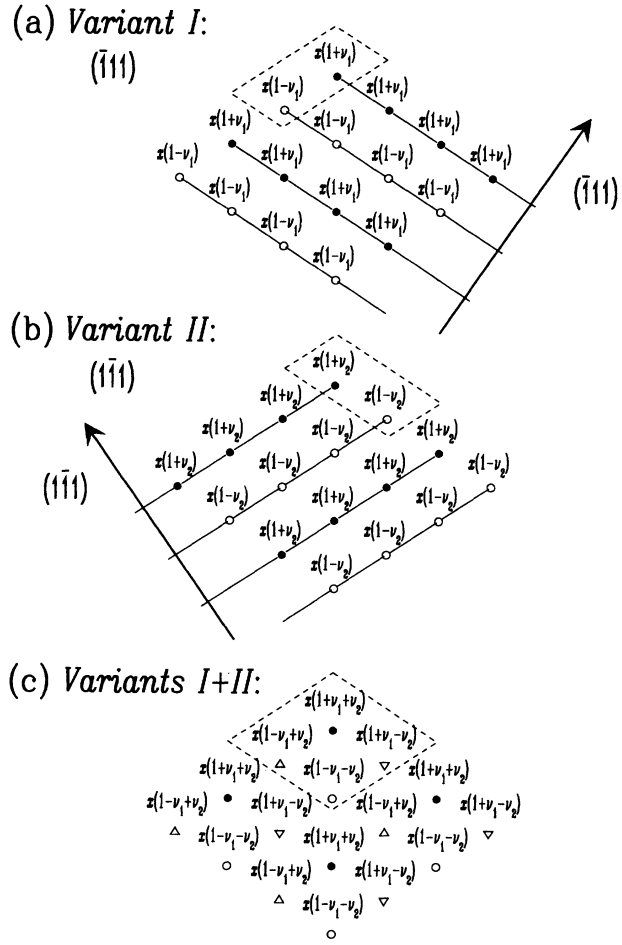

FIG. 5. Schematic illustration of interpenetration of two variants of ordering. The cross section of the crystal by the plane (110), parallel to both $[\bar{1}11]$ and $[1\bar{1}1]$ ordering axes is shown. (a) Average compositions $x(1+\nu_1)$ and $x(1-\nu_1)$ of the atomic rows perpendicular to the plane of the figure are shown for variant I; (b) the same for variant II. (c) Compositions of the same atomic rows in the double-ordered region. Dashed lines show the elementary cells in each case.

ν_1, ν_2 denote the ordering parameters for each variant. It is seen from Fig. 5(c) that within the double-ordered region these parameters should satisfy the condition $\nu_1 + \nu_2 \leq 1$. In particular, this means that within the double-ordered region the full ordering in one variant is impossible.

The electronic spectrum in the double-ordered region can be easily found using the approach of Sec. II. By analogy to Eq. (8) the ordering-induced perturbation of potential can be written as

$$\overline{\delta\Phi(\mathbf{r})} = \nu_1 x e^{i\boldsymbol{\sigma}_1\cdot\mathbf{r}} P_1(\mathbf{r}) + \nu_2 x e^{i\boldsymbol{\sigma}_2\cdot\mathbf{r}} P_2(\mathbf{r}) \tag{36}$$

with the wave vectors $\boldsymbol{\sigma}_1$ and $\boldsymbol{\sigma}_2$ corresponding to each variant of ordering. The functions P_1 and P_2 having the periodicity of the crystal are defined by Eq. (9) with $\boldsymbol{\sigma} = \boldsymbol{\sigma}_1$ and $\boldsymbol{\sigma} = \boldsymbol{\sigma}_2$, respectively. The perturbation (36) couples the Γ minimum with both L_1 and L_2 minima.

Thus we search for the wave function in the form

$$\Psi(\mathbf{r}) = e^{i\mathbf{k}\cdot\mathbf{r}}[u_\Gamma(\mathbf{r}) + \lambda_{\mathbf{k}}^1 e^{i\boldsymbol{\sigma}_1\cdot\mathbf{r}} u_{L_1}(\mathbf{r}) + \lambda_{\mathbf{k}}^2 e^{i\boldsymbol{\sigma}_2\cdot\mathbf{r}} u_{L_2}(\mathbf{r})] \tag{37}$$

with two coupling coefficients $\lambda_{\mathbf{k}}^1$ and $\lambda_{\mathbf{k}}^2$.

Performing the procedure analogous to that in Sec. II, we obtain the following system for the coupling coefficients $\lambda_{\mathbf{k}}^{1,2}$ and the spectrum $E(\mathbf{k})$:

$$[\varepsilon_\Gamma(\mathbf{k}) - E(\mathbf{k})] + \lambda_{\mathbf{k}}^1 V_1 + \lambda_{\mathbf{k}}^2 V_2 = 0, \tag{38a}$$

$$\lambda_{\mathbf{k}}^1[\varepsilon_{L_1}(\mathbf{k}) - E(\mathbf{k})] + V_1^* = 0, \tag{38b}$$

$$\lambda_{\mathbf{k}}^2[\varepsilon_{L_2}(\mathbf{k}) - E(\mathbf{k})] + V_2^* = 0, \tag{38c}$$

where V_1 and V_2 are the coupling parameters for each variant, defined by Eq. (14) with $P = P_1$ and $P = P_2$, respectively; $\varepsilon_{L_1}(\mathbf{k} - \boldsymbol{\sigma}_1)$ and $\varepsilon_{L_2}(\mathbf{k} - \boldsymbol{\sigma}_2)$ are the energy spectra of L_1 and L_2 minima. As in Sec. III, we mean by V_1 and V_2 the corresponding absolute values.

For simplicity we will not take into account the anisotropy of the L minima and assume

$$\varepsilon_{L_1}(\mathbf{k}) = \varepsilon_{L_2}(\mathbf{k}) = W + \frac{\hbar^2 k^2}{2m_L} = \varepsilon_L(k). \tag{39}$$

In this case two branches of the spectrum are given by Eq. (15), with V^2 replaced by $V_1^2 + V_2^2$:

$$\widetilde{E}_{\pm}(\mathbf{k}) = \frac{\varepsilon_\Gamma(\mathbf{k}) + \varepsilon_L(\mathbf{k})}{2} \pm \sqrt{\left(\frac{\varepsilon_\Gamma(\mathbf{k}) - \varepsilon_L(\mathbf{k})}{2}\right)^2 + V_1^2 + V_2^2}. \quad (40)$$

The third branch of the electronic spectrum, which we will denote as $E_0(\mathbf{k})$, remains unshifted and equal to the unperturbed energy of the L minima:

$$E_0(\mathbf{k}) = W + \frac{\hbar^2 k^2}{2m_L}. \quad (41)$$

The corresponding wave function has no admixture of $u_\Gamma(\mathbf{r})$:

$$\Psi_0(\mathbf{r}) = e^{i\mathbf{k}\cdot\mathbf{r}}[e^{i\boldsymbol{\sigma}_1\cdot\mathbf{r}}u_{L_1}(\mathbf{r}) - e^{i\boldsymbol{\sigma}_2\cdot\mathbf{r}}u_{L_2}(\mathbf{r})]. \quad (42)$$

The main consequence of the result obtained is that an overlapping between two domains with different variants of ordering results in an additional band-gap reduction compared to the band-gap reduction outside the region of overlapping. For equal ordering parameters $\nu_1 = \nu_2 = \nu$ this additional reduction is given by

$$\delta E_{\text{add}} = \sqrt{\left(\frac{W}{2}\right)^2 + 2V^2} - \sqrt{\left(\frac{W}{2}\right)^2 + V^2}, \quad (43)$$

where the matrix element V corresponds to the single variant of ordering. Therefore the region of the interpenetration of two variants, if it exists, represents a quantum well.

The size quantization in such a well exhibits nontrivial behavior. In contrast to the conventional case, when the bound state exists in the well of arbitrary small width, there is a threshold width for the first level to appear. The origin of such a threshold can be understood by considering the situation of zero width of the well, i.e., when the two variants are separated by a plane boundary. Note that if $\nu_1 = \nu_2$, the band structures to the left and to the right of such a boundary are completely identical so that there is no band offset. However, the Bloch functions in the left half-space represents the combinations of u_Γ and u_{L_1}, whereas the Bloch functions in the right half-space are the combination of u_Γ and u_{L_2}. As a result, a simple interdomain boundary should scatter an incident electron. The reason for the scattering is the difference in the Bloch functions corresponding to the same energy in the left and in the right half-spaces. This difference causes the effective asymmetry of the potential well which results in a finite threshold thickness for size quantization.

It seems instructive to study the reflection from the boundary between two domains. The specific of this problem is that an incident electron wave belonging to the branch $E_-(\mathbf{k})$ cannot be just reflected into the state of the same branch only. The reason is that one needs to match the envelope functions of u_Γ, u_{L_1}, and u_{L_2} at the boundary $x = 0$. As a result, the reflected and transmitted waves must represent the combinations of waves belonging to three branches: $E_-(\mathbf{k})$, $E_+(\mathbf{k})$, and the unperturbed branch $\varepsilon_L(k)$.

We consider the energy of the incident electron lying within the interval $-\delta E < E < W$. In this range only the lower branch component of the wave function represents the propagating wave. Two other components decay with the distance $|x|$ from the boundary. Therefore we can write the wave function in the left half-space ($x < 0$) as

$$\Psi(\mathbf{r}) = (e^{ik_- x} + Se^{-ik_- x})[u_\Gamma(\mathbf{r})\lambda_{k_-}e^{i\boldsymbol{\sigma}_1\cdot\mathbf{r}}u_{L_1}(\mathbf{r})] + A_l e^{\varkappa_+ x}[u_\Gamma(\mathbf{r}) + \lambda_{k_+}e^{i\boldsymbol{\sigma}_1\cdot\mathbf{r}}u_{L_1}(\mathbf{r})] + B_l e^{\varkappa_L x}e^{i\boldsymbol{\sigma}_2\cdot\mathbf{r}}u_{L_2}(\mathbf{r}), \quad (44)$$

whereas the wave function in the right half-space has the form

$$\Psi(\mathbf{r}) = Te^{ik_- x}[u_\Gamma(\mathbf{r}) + \lambda_{k_-}e^{i\boldsymbol{\sigma}_2\cdot\mathbf{r}}u_{L_2}(\mathbf{r})] + A_r e^{-\varkappa_+ x}[u_\Gamma(\mathbf{r}) + \lambda_{k_+}e^{i\boldsymbol{\sigma}_2\cdot\mathbf{r}}u_{L_2}(\mathbf{r})] + B_r e^{-\varkappa_L x}e^{i\boldsymbol{\sigma}_1\cdot\mathbf{r}}u_{L_1}(\mathbf{r}). \quad (45)$$

Here A_l, A_r and B_l, B_r are the amplitudes of the components from the branches $E_+(\mathbf{k})$ and $\varepsilon_L(k)$, respectively. T and S are the amplitudes of the transmitted and reflected waves.

Matching the envelope functions with their derivatives at the boundary $x = 0$ we obtain the linear system of six equations for six amplitudes T, S, A_l, A_r, B_l, B_r, similar to Eq. (29). The energy dependence of the reflection coefficient $R = |S|^2$ obtained from this system is shown in Fig. 6. We see that when the kinetic energy $E - E_-(0)$ tends to zero, the total reflection occurs as if the boundary represented a potential step. With increasing energy the reflection coefficient falls off within the range ε_0 given by

$$\varepsilon_0 = \frac{V^4}{4W^3}\left(\frac{m_\Gamma}{m_L}\right) \quad \text{for } V \ll W \quad (46)$$

and

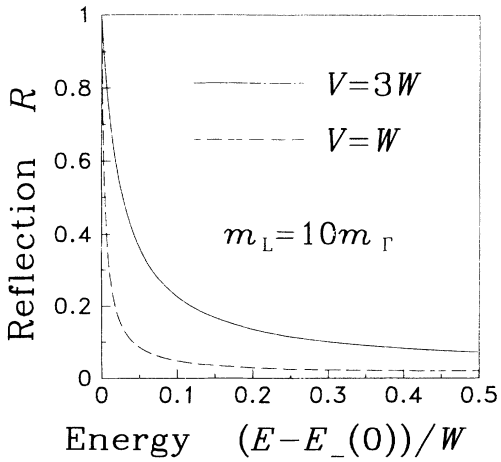

FIG. 6. Energy dependence of the reflection coefficient from the boundary between two domains with different variants of ordering.

$$\varepsilon_0 = W\left(\frac{m_\Gamma}{m_L}\right) \quad \text{for } V \gg W. \tag{47}$$

The energy interval ε_0 is much smaller than W because of the large difference between m_L and m_Γ. Reflectance disappears for all energies in the limit $m_L/m_\Gamma \to \infty$. This occurs since the contributions of the upper branches of the spectrum to the formation of the electronic wave function vanish according to the increase of the decay constants $æ_L$ and $æ_+$ in this limit.

Consider now the size quantization in the region of overlapping $|x| < d/2$ (Fig. 7). The wave function outside the well has the form similar to that studied above [see Eqs. (44), (45)]. The only difference is that for $E < 0$ all three components of the wave function decay with $|x|$. Hence, the wave function for $x < -d/2$ can be written in the form

$$\begin{aligned}\Psi(\mathbf{r}) = {} & D_- e^{æ_- x}[u_\Gamma(\mathbf{r}) + \lambda_{\mathbf{k}_-} e^{i\sigma_1\cdot\mathbf{r}} u_{L_1}(\mathbf{r})] \\ & + D_+ e^{æ_+ x}[u_\Gamma(\mathbf{r}) + \lambda_{\mathbf{k}_+} e^{i\sigma_1\cdot\mathbf{r}} u_{L_1}(\mathbf{r})] \\ & + D_0 e^{æ_L x} e^{i\sigma_2\cdot\mathbf{r}} u_{L_2}(\mathbf{r}).\end{aligned} \tag{48}$$

Here D_-, D_+, and D_0 are the numerical coefficients. The decay constants $æ_L$ and $æ_\pm$ ($æ_\pm^2 = -k_\pm^2 > 0$) can be obtained from Eqs. (25b) and (27). It can be seen that all levels in the double-ordered well can be classified as "even" and "odd." Namely for the region $x > d/2$ we can write

$$\begin{aligned}\Psi(\mathbf{r}) = \pm\{ & D_- e^{-æ_- x}[u_\Gamma(\mathbf{r}) + \lambda_{\mathbf{k}_-} e^{i\sigma_2\cdot\mathbf{r}} u_{L_2}(\mathbf{r})] \\ & + D_+ e^{-æ_+ x}[u_\Gamma(\mathbf{r}) + \lambda_{\mathbf{k}_+} e^{i\sigma_2\cdot\mathbf{r}} u_{L_2}(\mathbf{r})] \\ & - D_0 e^{-æ_L x} e^{i\sigma_1\cdot\mathbf{r}} u_{L_1}(\mathbf{r})\},\end{aligned} \tag{49}$$

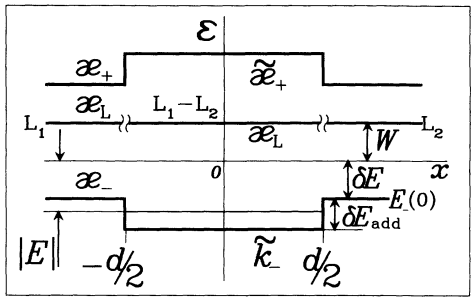

FIG. 7. Schematic band profile in the region of interpenetration of two variants of ordering. The energy E of the size quantization level is measured from the bottom of the conduction band in the disordered material. $E_-(0)$ is the bottom of the conduction band in the single-ordered material.

where the plus or minus sign should be chosen for even or odd states, respectively. Note that for the state we call even the third component of the wave function is odd. This fact is the consequence of the actual asymmetry of the well, discussed above. Correspondingly, for the odd states the third component of the wave function is even.

The wave function inside the well is a linear combination of three functions corresponding to the three branches $\tilde{E}_-(k)$, $\tilde{E}_+(k)$, and $E_0(k)$ of the spectrum of the double-ordered region. Corresponding wave numbers $\tilde{k}_-$, $\tilde{k}_+$, and k_0 should be obtained from the solution of the equations $\tilde{E}_-(\tilde{k}_-) = E$, $\tilde{E}_+(\tilde{k}_+) = E$, and $E_0(k_0) = E$, respectively. The dispersion laws $\tilde{E}_-(k) = E$ and $\tilde{E}_+(k) = E$ are defined by Eq. (39). The solutions for $\tilde{k}_-$ and $\tilde{k}_+$ are similar to Eq. (27) and have the form

$$\tilde{k}_\pm^2 = -\frac{1}{\hbar^2}\left\{m_\Gamma|E| + m_L(|E| + W) \pm \sqrt{[m_\Gamma|E| - m_L(|E| + W)]^2 + 8m_\Gamma m_L V^2}\right\}. \tag{50}$$

The value $k_0^2 = -æ_L^2$ is negative in the energy region under consideration.

The expression for the wave function of an even level inside the well can be written as

$$\begin{aligned}\Psi(\mathbf{r}) = {} & C_- \cos(k_- x)\{u_\Gamma(\mathbf{r}) + \lambda_{\mathbf{k}_-}[e^{i\sigma_1\cdot\mathbf{r}} u_{L_1}(\mathbf{r}) + e^{i\sigma_2\cdot\mathbf{r}} u_{L_2}(\mathbf{r})]\} \\ & + C_+ \cosh(æ_+ x)\{u_\Gamma(\mathbf{r}) + \lambda_{\mathbf{k}_+}(e^{i\sigma_1\cdot\mathbf{r}} u_{L_1}(\mathbf{r}) + e^{i\sigma_2\cdot\mathbf{r}} u_{L_2}(\mathbf{r})]\} + C_0 \sinh(æ_L x)[e^{i\sigma_1\cdot\mathbf{r}} u_{L_1}(\mathbf{r}) - e^{i\sigma_2\cdot\mathbf{r}} u_{L_2}(\mathbf{r})].\end{aligned} \tag{51}$$

Note that in order to satisfy the boundary conditions at $x = \pm d/2$, the envelope function of the third component is chosen to be odd. For the odd state one should replace cos, cosh, and sinh by sin, sinh, and cosh, respectively.

Matching the envelope functions and their derivatives at the boundary $x = d/2$ we find the linear system for the coefficients D_-, D_+, D_0, C_-, C_+, and C_0. The equation for the energy level positions can be found by equating to zero the determinant of the system. The numerical solutions of these equations for different degrees of ordering V/W and different mass ratios m_Γ/m_L are shown in Fig. 8. For comparison, the positions of energy levels for an electron with mass m_Γ in the regular potential well of the same width d and depth δE_{add} are shown.

It is seen that the energy levels are lower than in the regular well. This is the consequence of the fact that the effective mass corresponding to the branch $E_-(k)$ is larger than m_Γ. However, the difference is not as strong as in the case of the ordered layer studied in Sec. III. Even in the case of strong ordering the decrease in the energy level positions compared to those in the regular well is about 30%.

Figures 8(a)–8(c) show the existence of the threshold width for the first level. The energy level positions for

small d are shown in detail in Fig. 8(d). The threshold disappears in the limit $m_L/m_\Gamma \to \infty$. The reason for that is exactly the same as for the disappearance of the reflectance from the simple interdomain boundary in the same limit.

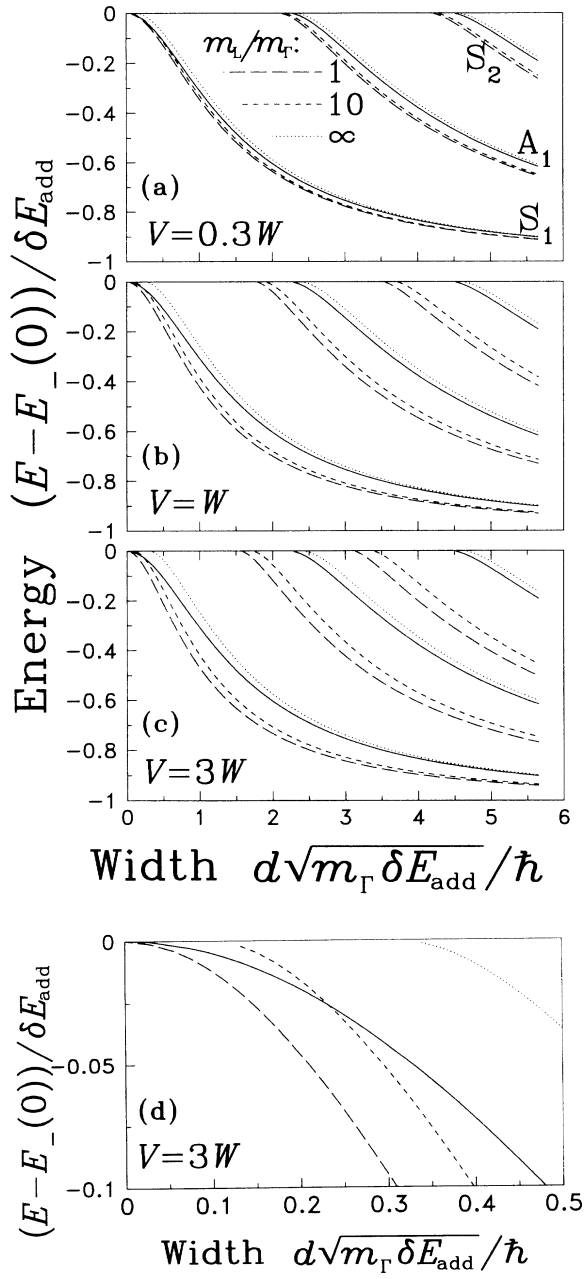

FIG. 8. Energy positions of the first three size quantization levels in the double-ordered region, calculated for different mass ratios m_L/m_Γ and degrees of ordering (a) $V = 0.3W$, (b) $V = W$, and (c) $V = 3W$; S and A stand for symmetrical (even) and antisymmetrical (odd) states, respectively. Solid lines show the positions of the energy levels in the regular potential well of the width d and depth δE_{add}; (d) the threshold behavior of the level S_1 as a function of width d is shown for $V = 3W$.

V. CONCLUSION

In the present paper a simple analytical theory of the conduction-band spectrum in partially ordered semiconductor alloys is developed. In our calculations we described the ordering by the change in the crystalline potential in each sub-sublattice, neglecting the change in the lattice constant due to ordering. Taking this effect into account may result in additional shifts in the band-edge positions. We did not estimate this shift since we have not found in the literature the corresponding deformation potential for the conduction band. The important point, however, is that the form of the energy spectrum will not change, since such a shift will cause only the renormalization of the parameter W.

Our theory predicts the existence of two branches of the conduction-band spectrum, spaced in energy by relatively small interval $\sqrt{W^2+4V^2}$. For strong ordering $V \gg W$ these branches are almost parallel. Such a picture is also supported by the numerical calculations performed by Kurimoto, Hamada, and Oshiyama in Ref. 53 (see also Ref. 52). In this paper the band structure of (111) $InGaP_2$ superlattice was calculated. Note that such a superlattice can be viewed as a completely ordered $In_{0.5}Ga_{0.5}P$. The calculations show the presence of two nearly parallel branches spaced by ~ 900 meV. This allows us to estimate the parameter V for full ordering ($\nu = 1$) as $V_{max} \approx 450$ meV. The value of V_{max} can be also estimated using the table of band gaps in ordered alloys calculated by Wei and Zunger in Ref. 49. Taking the band-gap reduction $\delta E = 260$ meV we obtain $V_{max} = \sqrt{\delta E(W+\delta E)} \approx 320$ meV, which is about 30% smaller.

In our consideration we assumed the disordered material to have a direct gap. Our results for the energy spectrum, however, apply also for indirect alloys with the L minimum lower than the Γ minimum. In this case the value of the parameter W is negative. Note that ordering in indirect materials causes nonzero matrix element for the optical transition between the minima of the conduction and valence bands. This occurs due to the admixture of u_Γ to the Bloch function of the bottom of conduction band. This admixture is proportional to the ordering parameter ν for $V \ll |W|$ and it saturates when $V \sim |W|$.

Experiments using transmission electron microscopy frequently indicate the presence of two variants of ordering within one sample (see, for example, Refs. 4, 7, 17, and 18). In the present paper we have considered three plausible situations. (i) Domains with different variants are surrounded by the disordered region so that there is no contact between them. In this case each domain represents a quantum well. (ii) Domains with different variants of ordering have common boundary. We have shown that, although such a boundary is not associated with any potential jump, it behaves as a scatterer for an incident electron. (iii) Domains with different variants of ordering overlap. We have shown that the region of overlapping represents a quantum well. As follows from Eqs. (16) and (43), the depth of the well in the case

of strong ordering is about 70% of the band-gap reduction in a single-ordered region. Electronic states in such a well should manifest themselves as a peak in the low-energy region of the luminescence spectrum. Note that the existence of these states is an intrinsic property of the structure and is not related to defects or any statistical or technological disorder. Important is that the low-energy part of the luminescence spectrum caused by these states should be absent in the samples with the single variant of ordering.

ACKNOWLEDGMENTS

We are grateful to P. C. Taylor and M. C. DeLong for valuable discussions. We are also grateful to W. D. Ohlsen for reading the manuscript and useful remarks.

* Permanent address: A. F. Ioffe Physical-Technical Institute, St. Petersburg, Russia.

[1] T. S. Kuan, W. I. Wang, and E. L. Wilkie, Appl. Phys. Lett. **51**, 51 (1987).
[2] M. A. Shahid, S. Mahajan, D. E. Laughlin, and H. M. Cox, Phys. Rev. Lett. **58**, 2567 (1987).
[3] S. N. G. Chu, R. A. Logan, and T. Tanbun-Ek, J. Appl. Phys. **72**, 4118 (1992).
[4] G. B. Stringfellow and G. S. Chen, J. Vac. Sci. Technol. B **9**, 2182 (1991).
[5] G. S. Chen, D. H. Jaw, and G. B. Stringfellow, Appl. Phys. Lett. **57**, 2475 (1990).
[6] G. S. Chen, D. H. Jaw, and G. B. Stringfellow, J. Appl. Phys. **69**, 4263 (1991).
[7] G. S. Chen and G. B. Stringfellow, Appl. Phys. Lett. **59**, 3258 (1991).
[8] W. E. Plano, D. W. Nam, J. S. Major, Jr., K. C. Hsieh, and N. Holonyak, Jr., Appl. Phys. Lett. **53**, 2537 (1988).
[9] H. R. Jen, K. Y. Ma, and G. B. Stringfellow, Appl. Phys. Lett. **54**, 1154 (1989).
[10] D. H. Jaw, G. S. Chen, and G. B. Stringfellow, Appl. Phys. Lett. **59**, 114 (1991).
[11] T. S. Kuan, T. F. Kuech, W. I. Wang, and E. L. Wilkie, Phys. Rev. Lett. **54**, 201 (1985).
[12] P. M. Petroff, A. Y. Cho, F. K. Reinhart, A. C. Gossard, and W. Wiegmann, Phys. Rev. Lett. **48**, 170 (1982).
[13] A. G. Norman, R. E. Mallard, I. J. Murgatroyd, G. R. Booker, A. H. Moore, and M. D. Scott, in *Microscopy of Semiconductor Materials, Proceedings of the Institute of Physics Conference, Oxford, UK, April 1987*, IOP Conf. Proc. No. 87 (Institute of Physics and Physical Society, London, 1987), p. 77.
[14] J. R. Passetto and G. B. Stringfellow, J. Cryst. Growth **65**, 454 (1983); **98**, 108 (1989).
[15] Y.-E. Ihm, N. Otsuka, J. Klem, and H. Morkoc, Appl. Phys. Lett. **51**, 2013 (1987).
[16] S. Yasuami, C. Nozaki, and Y. Ohba, Appl. Phys. Lett. **52**, 2031 (1988).
[17] G. S. Chen and G. B. Stringfellow, Appl. Phys. Lett. **59**, 324 (1991).
[18] D. S. Cao, E. H. Reihlen, G. S. Chen, A. W. Kimball, and G. B. Stringfellow, J. Cryst. Growth **109**, 279 (1991).
[19] S. R. Kurtz, J. M. Olson, and A. Kibbler, Appl. Phys. Lett. **57**, 1922 (1990).
[20] D. J. Friedman, J. G. Zhu, A. E. Kibbler, J. M. Olson, and J. Moreland, Appl. Phys. Lett. **63**, 1774 (1993).
[21] B. T. McDermott, K. G. Reid, N. A. El-Masry, and S. M. Bedair, Appl. Phys. Lett. **56**, 1172 (1990).
[22] S. R. Kurtz, J. M. Olson, and A. Kibbler, Appl. Phys. Lett. **45**, 718 (1989).
[23] A. Gomyo, T. Suzuki, and S. Iijima, Phys. Rev. Lett. **60**, 2645 (1988).
[24] P. Bellon, J. P. Chevalier, G. P. Martin, E. Dupont-Nivet, C. Thiebaut, and J. P. Andre, Appl. Phys. Lett. **52**, 567 (1988).
[25] F. P. Dabkowski, P. Gavriolic, K. Meehan, W. Stutius, J. E. Williams, M. A. Shahid, and S. Mahajan, Appl. Phys. Lett. **52**, 2142 (1988).
[26] A. Mascarenhas, S. Kurtz, A. Kibbler, and J. M. Olson, Phys. Rev. Lett. **63**, 2108 (1989).
[27] D. J. Mowbray, R. A. Hogg, M. S. Skolnick, M. C. DeLong, S. R. Kurtz, and J. M. Olson, Phys. Rev. B **46**, 7232 (1992).
[28] G. W. 't Hooft, C. J. B. Riviere, M. P. C. M. Krijn, and C. T. H. F. Liedenbaum, Appl. Phys. Lett. **61**, 3169 (1992).
[29] T. Kanata, M. Nishimoto, H. Nakayama, and T. Nishino, Phys. Rev. B **45**, 6637 (1992).
[30] M. C. DeLong, D. J. Mowbray, R. A. Hogg, and M. S. Skolnick, M. Hopkinson, J. P. R. David, P. C. Taylor, S. R. Kurtz, and J. M. Olson, J. Appl. Phys. **73**, 5163 (1993).
[31] R. P. Schneider, Jr., E. D. Jones, J. A. Lott, and R. P. Bryan, J. Appl. Phys. **72**, 5397 (1992).
[32] R. H. Horng, L. C. Haung, and M. K. Lee, Mater. Chem. Phys. **32**, 73 (1992).
[33] J. E. Fouquet, V. M. Robbins, J. Rosner, and O. Blum, Appl. Phys. Lett. **57**, 1566 (1990).
[34] T. Nishino, Y. Inoue, and Y. Hamakawa, Appl. Phys. Lett. **53**, 583 (1988).
[35] Y. Inoue, T. Nishino, Y. Hamakawa, M. Kondow, and S. Minagawa, Opto-electron. Devices Technol. **3**, 61 (1988).
[36] S. R. Kurtz, J. M. Olson, and A. Kibbler, Solar Cells **24**, 307 (1988).
[37] M. K. Lee, R. H. Horng, and L. C. Haung, J. Appl. Phys. **72**, 5420 (1992).
[38] K. Nakano, A. Toda, T. Yamamoto, and A. Ishibashi, Appl. Phys. Lett. **61**, 1959 (1992).
[39] G. P. Srivastava, J. L. Martins, and A. Zunger, Phys. Rev. B **31**, 2561 (1984).
[40] S.-H. Wei and A. Zunger, Phys. Rev. Lett. **61**, 1505 (1988).
[41] J. E. Bernard, S. Froyen, and A. Zunger, Phys. Rev. B **44**, 11 178 (1991).
[42] R. Osorio, J. E. Bernard, S. Froyen, and A. Zunger, Phys. Rev. B **45**, 11 173 (1992).
[43] J. E. Bernard, L. G. Ferreira, S.-H. Wei, and A. Zunger, Phys. Rev. B **38**, 6338 (1988).
[44] A. Zunger and D. M. Wood, J. Cryst. Growth **98**, 1 (1989).
[45] A. A. Mbaye, L. G. Ferreira, and A. Zunger, Phys. Rev. Lett. **58**, 49 (1987).
[46] B. Gu and J. Ni, J. Phys. Condens. Matter **4**, 9339 (1992).
[47] R. Magri and C. Calandra, Phys. Rev. B **40**, 3896 (1989).
[48] S.-H. Wei and A. Zunger, Phys. Rev. B **39**, 3279 (1989).
[49] S.-H. Wei and A. Zunger, Appl. Phys. Lett. **56**, 662 (1990).
[50] S.-H. Wei and A. Zunger, Appl. Phys. Lett. **53**, 2077 (1988).
[51] R. B. Capaz and B. Koiller, Phys. Rev. B **47**, 4044 (1993).
[52] T. Kurimoto and N. Hamada, Phys. Rev. B **40**, 3889 (1989).

[53] T. Kurimoto, N. Hamada, and A. Oshiyama, Superlatt. Microstruct. **5**, 171 (1989).

[54] *Numerical Data and Functional Relationships in Science and Technology*, edited by O. Madelung, Landolt-Börnstein, New Series, Group III, Vol. 17, Pts. a and b (Springer-Verlag, Berlin, 1982).

[55] A. L. Efros and M. E. Raikh, in *Optical Properties of Mixed Crystals*, edited by R. J. Elliott and I. P. Ipatova (North-Holland, Amsterdam, 1988), p. 135.